

# Nonequilibrium free energy and information flow of a double quantum-dot system with Coulomb coupling

Zhiyuan Lin, Tong Fu, Juying Xiao, Shanhe Su,<sup>\*</sup> and Jincan Chen

*Department of Physics, Xiamen University,  
Xiamen 361005, People's Republic of China*

Yanchao Zhang<sup>†</sup>

*School of Science, Guangxi University of Science and Technology,  
Liuzhou 545006, People's Republic of China*

## Abstract

We build a double quantum-dot system with Coulomb coupling and aim at studying the connections among the entropy production, free energy, and information flow. By utilizing the concepts in stochastic thermodynamics and graph theory analysis, the Clausius and nonequilibrium free energy inequalities are built to interpret the local second law of thermodynamics for subsystems. A fundamental set of cycle fluxes and affinities is identified to decompose the two inequalities by using Schnakenberg's network theory. The results show that the thermodynamic irreversibility has the energy-related and information-related contributions. A global cycle associated with the feedback-induced information flow would pump electrons against the bias voltage, which implements a Maxwell Demon.

---

<sup>\*</sup>Electronic address: shanhesu@xmu.edu.cn

<sup>†</sup>Electronic address: zhangyanchao@gxust.edu.cn

## I. INTRODUCTION

Irreversible thermodynamics is an extension of thermodynamics that studies the transport phenomena such as the exchanges of mass, energy, and charge [1]. The Onsager reciprocity theorem expresses the rate of entropy production as the sum of the products of each flux and its conjugate affinity [2, 3]. This thermodynamic relation is applicable for most far-from-equilibrium systems, even without accounting for the linear response regime. A nonzero affinity implies that a system is not in equilibrium and irreversible processes drive the system towards the state of equilibrium. The criterion for the selection of the basic thermodynamic flows and forces remains a question worth exploring. For instance, the rate of entropy production of a thermoelectric device can be equivalently expressed in energy and heat representations [4]. Instead of collecting flows according to the thermodynamic forces acting in the energy transduction, biogeochemical systems adopt the basic graph concepts used in network analysis [5].

Graph theory analysis indicates that each cycle makes an additive positive contribution to the total rate of entropy production in the ensemble [6]. Schnakenberg expressed the macroscopic entropy production of stochastic processes in terms of the cycles from the network, because the products of the transition rates along a cycle depend only on the macroscopic thermodynamic affinities maintaining the system out of equilibrium [7]. Horowitz et al. used a graph theoretic method to provide a unified thermodynamic scheme describing information transfers in autonomous systems [8]. Yamamoto introduced a graph contraction method to prove that the Onsager coefficient associated with the driving of an information current satisfies the Onsager reciprocity [9]. Graph theory concepts have achieved great success at learning irreversible thermodynamics of the energy [10, 11], entropy, fluctuation [12], and information at nanoscale [13, 14].

On the one hand, many studies were concerned with the formalism of free energy for irreversible thermodynamics. Crooks related nonequilibrium measurements of free energy differences to the work done on microscopically reversible Markovian systems [15, 16]. The Jarzynski relation, which relates the free energy differences between two states to the irreversible work along an ensemble of trajectories joining the same states, has been often used for calculating the equilibrium free energies of classical and quantum systems [17–20]. Esposito introduced the concept of nonequilibrium system free energy to understand the irreversible

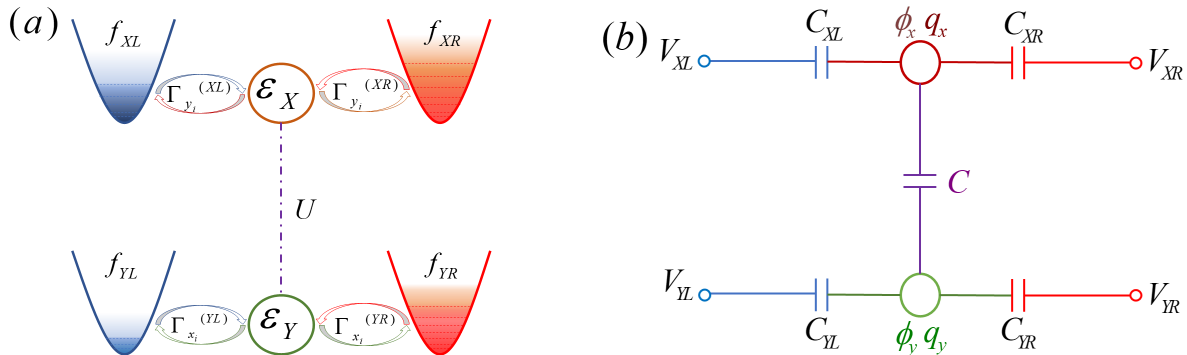


Figure 1: (a) The Schematic diagram of a Coulomb-coupled double quantum-dot system. (b) The equivalent circuit showing the capacitive couplings between the quantum dots and the reservoirs.

work in Hamiltonian dynamics of an open driven system [21, 22]. More recently, the investigations of free energy were generalized to the systems coupled to the environment with multiple heat baths [23–26]. More and More studies utilized the nonequilibrium Clausius and free energy inequalities to clarify the information and energy regimes in the nonequilibrium systems [27–35]. Miyahara et al. derived the Sagawa-Ueda-Jarzynski relation under a nonisothermal system to measure the change of the free energy [26]. Ptaszyński et al. formulated a nonequilibrium free energy inequality for a generic open quantum system weakly coupled to multi heat sources [23]. Despite recent developments, relatively little attention has been paid to correlate the non-equilibrium free energy in terms of thermodynamic affinities and flows. By considering the great success of graph theory analysis in irreversible thermodynamics, a cycle decomposition may help to establish this connection.

Considering a double-quantum-dot system, we will employ graph theory to analyze the entropy production and the non-equilibrium free energy of the open quantum system obeying continuous-time Markov jump process. The contents are organized as follows: In Section II, the general model of two quantum dots coupled in parallel to four electronic reservoirs with different chemical potentials is briefly described. Schnakenberg’s network theory are applied to obtain the fundamental cycle fluxes and affinities. The nonequilibrium Clausius and free energy inequalities of the subsystems at steady state are derived. In Section III, the main thermodynamic characteristic functions as functions of the Coulomb coupling strength will be evaluated numerically. Finally, the main conclusions are drawn.

## II. MODEL AND METHODS

### A. *The double quantum-dot system with Coulomb coupling*

The considered model is a bipartite system that consists of capacitively coupled quantum dots  $X$  and  $Y$ , as shown in Fig. 1 (a). The quantum dots  $X$  and  $Y$  with energies  $\varepsilon_X$  and  $\varepsilon_Y$  are coupled via the long-range Coulomb force  $U$  such that they only exchange energy but no electrons. The states of the composite system are given by a four-state basis  $z = \{|(x_0, y_0)\rangle, |(x_1, y_0)\rangle, |(x_0, y_1)\rangle, |(x_1, y_1)\rangle\}$ , where  $x_0$  and  $y_0$  ( $x_1$  and  $y_1$ ) represent that the site of  $X$  and  $Y$  is empty (filled), respectively. The quantum dot  $X$  ( $Y$ ) is connected to two Fermi reservoirs  $XL$  and  $XR$  ( $YL$  and  $YR$ ) and admits the electron transports through parallel interacting channels. Figure 1(b) is the equivalent circuit showing the capacitive couplings between the quantum dots and the reservoirs.  $V_\nu = \mu_\nu/e$  ( $\nu = XL, XR, YL, YR$ ) determines the voltage of the reservoir  $\nu$ , where  $\mu_\nu$  is the chemical potential and  $e$  is elementary positive charge. The imbalance capacitances between the quantum dot and the terminal  $\nu$  and between the quantum dots are defined as  $C_\nu$  and  $C$ , respectively.  $\phi_x$  and  $\phi_y$  are the electrostatic potentials in each quantum dot at state  $|(x, y)\rangle$ . The total charges of  $X$  and  $Y$  at state  $|(x, y)\rangle$  are the sum of the charges on all of the capacitors connected to  $X$  and  $Y$  [36, 37], i.e.,

$$q_x = C_{XL}(\phi_x - V_{XL}) + C_{XR}(\phi_x - V_{XR}) + C(\phi_x - \phi_y), \quad (1)$$

$$q_y = C_{YL}(\phi_y - V_{YL}) + C_{YR}(\phi_y - V_{YR}) + C(\phi_y - \phi_x). \quad (2)$$

These two equations can be expressed more compactly in a matrix form

$$\begin{bmatrix} q_x + C_{XL}V_{XL} + C_{XR}V_{XR} \\ q_y + C_{YL}V_{YL} + C_{YR}V_{YR} \end{bmatrix} = \begin{bmatrix} C'_X & -C \\ -C & C'_Y \end{bmatrix} \begin{bmatrix} \phi_x \\ \phi_y \end{bmatrix}, \quad (3)$$

where  $C'_X = C_{XL} + C_{XR} + C$  and  $C'_Y = C_{YL} + C_{YR} + C$  define the total capacitances of  $X$  and  $Y$ . The electrostatic potentials  $\phi_x$  and  $\phi_y$  are then conveniently expressed by using the capacitance matrix

$$\begin{bmatrix} \phi_x \\ \phi_y \end{bmatrix} = \frac{1}{C'_X C'_Y - C^2} \begin{bmatrix} C'_Y & C \\ C & C'_X \end{bmatrix} \begin{bmatrix} q_x + C_{XL}V_{XL} + C_{XR}V_{XR} \\ q_y + C_{YL}V_{YL} + C_{YR}V_{YR} \end{bmatrix}. \quad (4)$$

The electrostatic energy for a given quantum state is computed by

$$U(x, y) = \frac{1}{2} [q_x + C_{XL}V_{XL} + C_{XR}V_{XR}, q_y + C_{YL}V_{YL} + C_{YR}V_{YR}] \begin{bmatrix} \phi_x \\ \phi_y \end{bmatrix}. \quad (5)$$

Note that  $q_x (q_y) = 0$  or  $e$ , depending on whether  $X (Y)$  is empty or occupied. Thus, the electrostatic energies for the four quantum states read

$$\begin{aligned} U(x_0, y_0) &= \frac{1}{2(C'_X C'_Y - C^2)} (C'_Y \mathcal{Q}_x^2 + 2C \mathcal{Q}_x \mathcal{Q}_y + C'_X \mathcal{Q}_y^2), \\ U(x_1, y_0) &= \frac{1}{2(C'_X C'_Y - C^2)} [C'_Y (e^2 + 2e\mathcal{Q}_x) + 2eC \mathcal{Q}_y] + U_{x_0 y_0}, \\ U(x_0, y_1) &= \frac{1}{2(C'_X C'_Y - C^2)} [2eC \mathcal{Q}_x + C'_X (e^2 + 2e\mathcal{Q}_y)] + U_{x_0 y_0}, \\ U(x_1, y_1) &= \frac{2e^2 C}{2(C'_X C'_Y - C^2)} + U_{x_1 y_0} + U_{x_0 y_1} - U_{x_0 y_0}, \end{aligned} \quad (6)$$

where  $\mathcal{Q}_x = C_{XL}V_{XL} + C_{XR}V_{XR}$  and  $\mathcal{Q}_y = C_{YL}V_{YL} + C_{YR}V_{YR}$ . We are now capable of determining the change of energy in the system when an electron tunnels into a quantum dot. When the other dot is empty, the charging energies of  $X$  and  $Y$  are, respectively, given by

$$U_{X_0} = U(x_1, y_0) - U(x_0, y_0), U_{Y_0} = U(x_0, y_1) - U(x_0, y_0). \quad (7)$$

On the other hand, when the other dot is occupied, the charging energies of  $X$  and  $Y$  are, respectively, described by

$$U_{X_1} = U(x_1, y_1) - U(x_0, y_1), U_{Y_1} = U(x_1, y_1) - U(x_1, y_0). \quad (8)$$

The differences of the charging energies  $U_{X_1} - U_{X_0} = U_{Y_1} - U_{Y_0} = U$ , where  $U = \frac{q^2 C}{(C'_X C'_Y - C^2)}$  determines the quantized energy which can be transferred from one dot to the other dot.

## B. *The master equation*

Let  $p(z, t)$  be the probability of state  $z$  of the coupled quantum dots at time  $t$ . In the regime of sequential tunneling approximation, the broadening of energy levels can be neglected and the transmission through tunnel barriers is defined by the sequential tunneling

of a single electron. Thus, the time evolution of  $p(z, t)$  is governed by a Markovian master equation [38–40]

$$\frac{d}{dt}p(z, t) = \sum_{z', \nu} \left[ R_{zz'}^{(\nu)} p(z', t) - R_{z'z}^{(\nu)} p(z, t) \right]. \quad (9)$$

The transition rate from state  $z'$  to state  $z$  induced by the reservoir  $\nu$  reads

$$R_{zz'}^{(\nu)} = \begin{cases} R_{xx'|y}^{(\nu)} & (x \neq x', y = y', \nu = XL, XR) \\ R_{yy'|x}^{(\nu)} & (x = x', y \neq y', \nu = YL, YR) \\ 0 & (\text{otherwise}) \end{cases}, \quad (10)$$

where  $x' \in \{x_0, x_1\}$  and  $y' \in \{y_0, y_1\}$ . We have assumed that the two subsystems should not change their states simultaneously during a single transition process. The specific forms of the transition rates are

$$\begin{aligned} R_{x_1x_0|y_i}^{(\nu)} &= \Gamma_{y_i}^{(\nu)} f_{y_i}^{(\nu)}, \\ R_{x_0x_1|y_i}^{(\nu)} &= \Gamma_{y_i}^{(\nu)} (1 - f_{y_i}^{(\nu)}), \\ R_{y_1y_0|x_i}^{(\nu)} &= \Gamma_{x_i}^{(\nu)} f_{x_i}^{(\nu)}, \\ R_{y_0y_1|x_i}^{(\nu)} &= \Gamma_{x_i}^{(\nu)} (1 - f_{x_i}^{(\nu)}), \end{aligned} \quad (11)$$

where  $f_{x_i}^{(\nu)} = \{1 + \exp[\beta_\nu (\varepsilon'_Y + iU - \mu_\nu)]\}^{-1}$ ,  $f_{y_i}^{(\nu)} = \{1 + \exp[\beta_\nu (\varepsilon'_X + iU - \mu_\nu)]\}^{-1}$  ( $i = 0, 1$ ),  $\varepsilon'_X = \varepsilon_X + U_{X_0}$ , and  $\varepsilon'_Y = \varepsilon_Y + U_{Y_0}$ . The reservoir  $\nu$  is at temperature  $T_\nu$  and the chemical potential is  $\mu_\nu$ . All temperatures are set to be equal, i.e.,  $T_\nu = T$ . The inverse temperature parameter  $\beta_\nu = 1/(k_B T_\nu)$ , where  $k_B$  is Boltzmann's constant and we set  $k_B = 1$  in the discussion.  $\Gamma_{x_i}^{(\nu)}$  ( $\Gamma_{y_i}^{(\nu)}$ ) is a positive constant describing the height of the potential barrier between the dot  $Y(X)$  and the reservoir  $\nu$ . The potential barrier of  $Y$ , characterized by  $\Gamma_{x_i}^{(\nu)}$ , depends on the state of  $X$ , and vice versa.

### C. Schnakenberg's network theory

Schnakenberg stated that nonequilibrium random processes could be investigated and understood by carrying out the graph analysis associated with the master equation [9, 12, 41]. For purposes of relating the thermodynamic properties to the fundamental fluxes and

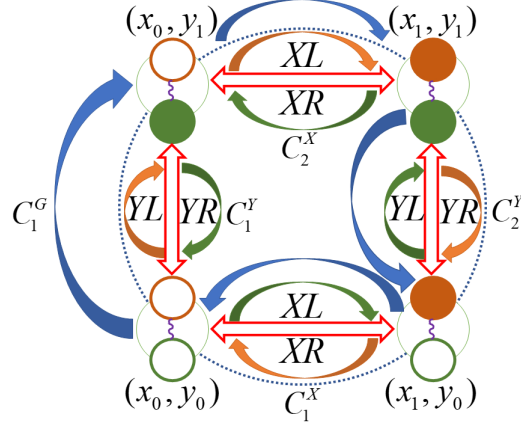


Figure 2: Illustration of the directed graph and the cycle basis. The vertices represent the four states of the two quantum dots, and the double-headed arrows stand for the forward and backward transitions between the two states induced by reservoirs. The single-headed curly arrows are the edges of a cycle basis with a directed orientation. Note that we can arbitrarily choose the direction of an edge.

affinities, a graph representation of the dynamics of the double quantum-dot system is introduced (Fig. 2).

According to Schnakenberg's network theory, a vertex in the graph represents a state of the system  $z$ . A directed edge  $e := (z' \xrightarrow{\nu} z)$  is corresponding to the transition from state  $z'$  to state  $z$  through the reservoir  $\nu$  with a nonzero transition rate  $R_{zz'}^{(\nu)}$ . For edge  $e$ , the edge affinity and edge current are identified as

$$\mathcal{F}_e = \ln \frac{R_{zz'}^{(\nu)}}{R_{z'z}^{(\nu)}}, \quad (12)$$

$$J_e = R_{zz'}^{(\nu)} p(z', t) - R_{z'z}^{(\nu)} p(z, t), \quad (13)$$

respectively. We next define the effective affinity of edge  $e$

$$\mathcal{F}_e := \mathcal{F}_e + \ln \frac{p(z', t)}{p(z, t)}. \quad (14)$$

Because  $J_e = 0$  resulting in  $\mathcal{F}_e = 0$ , the effective affinity acts as the conjugate of the current  $J_e$ . In contrast,  $\mathcal{F}_e$  can be regarded as the bare thermodynamic affinity related to the detailed balance.

According to Kirchhoff's current law [41], the stationary Master equation [Eq. (9) with  $\frac{d}{dt}p(z, t) = 0$ ] leads to

$$\sum_{z', \nu} J_e = 0. \quad (15)$$

By specifying the set  $\mathcal{E}$  as a collection of the directed edges (represented by the single-headed curly arrows) in Fig. 2, we have  $(z' \rightarrow z) \in \mathcal{E} \Rightarrow (z \rightarrow z') \notin \mathcal{E}$ . Under the assignment in Eq. (10), each edge only describes a transition in  $X$  or  $Y$ . Therefore, one can use the set  $\mathcal{E}^X := \left\{ e = \left( (x', y) \xrightarrow{\nu} (x, y) \right) \in \mathcal{E} \right\} (x \neq x')$  to describe the transitions in  $X$  and the other set  $\mathcal{E}^Y := \left\{ e = \left( (x, y') \xrightarrow{\nu} (x, y) \right) \in \mathcal{E} \right\} (y \neq y')$  to cover the transitions in  $Y$ . The set  $\mathcal{E}$  of all edges is then divided into two parts  $\mathcal{E}^X$  and  $\mathcal{E}^Y$ .

The cycle basis of the directed graph (Fig. 2)  $\mathcal{C} = \{C_1^X, C_2^X, C_1^G, C_1^Y, C_2^Y\}$  may be classified into the local and global cycles as

$$\begin{aligned} C_1^X &:= \left\{ (x_0, y_0) \xrightarrow{XL} (x_1, y_0) \xrightarrow{XR} (x_0, y_0) \right\}, \\ C_2^X &:= \left\{ (x_0, y_1) \xrightarrow{XL} (x_1, y_1) \xrightarrow{XR} (x_0, y_1) \right\}, \\ C_1^Y &:= \left\{ (x_0, y_0) \xrightarrow{YL} (x_0, y_1) \xrightarrow{YR} (x_0, y_0) \right\}, \\ C_2^Y &:= \left\{ (x_1, y_0) \xrightarrow{YL} (x_1, y_1) \xrightarrow{YR} (x_1, y_0) \right\}, \\ C_1^G &:= \left\{ (x_0, y_0) \xrightarrow{YL} (x_0, y_1) \xrightarrow{XL} (x_1, y_1) \xrightarrow{YR} (x_1, y_0) \xrightarrow{XR} (x_0, y_0) \right\}. \end{aligned} \quad (16)$$

A directed cycle is a directed sequence of the connected edges with the same initial and terminal vertexes. This set of cycles is broadly classified into three groups: local cycles of  $X$ ,  $\mathcal{C}^X := \{C_1^X, C_2^X\}$ ; local cycles of  $Y$ ,  $\mathcal{C}^Y := \{C_1^Y, C_2^Y\}$ ; and a global cycle,  $\mathcal{C}^G := \{C_1^G\}$ . A local cycle indicates that  $X$  ( $Y$ ) is fixed and  $Y$  ( $X$ ) is changing, which supports the internal subsystem flows. The global cycle  $C_1^G$  links  $X$  and  $Y$ , so that a current flowing around a global cycle carries energy and entropy from one subsystem to the other. Any other cycles are recognized as a linear combination of cycles in  $\mathcal{C}$  [8]. It will be useful to introduce the function

$$\Xi(e, C_k) := \begin{cases} 1 & (e \in C_k^l) \\ -1 & (e^\dagger \in C_k^l) \\ 0 & (\text{otherwise}) \end{cases}, \quad (17)$$

where  $e \in C_k^l$  ( $l = X, Y, G; k = 1, 2$ ) means that  $e$  is one of the edges in  $C_k^l$ , and  $e^\dagger := (z \xrightarrow{\nu} z')$  defines the backward transition edge of  $e$ . To each fundamental cycle, one can then assign the affinity  $\mathcal{F}(C_k^l)$  as a sum of the affinities along the edges in  $C_k^l$

$$\mathcal{F}(C_k^l) := \sum_{e \in \mathcal{E}} \Xi(e, C_k^l) \mathcal{F}_e. \quad (18)$$

The motive is to introduce the partial affinities of the cycles associated with  $X$  and  $Y$  by

$$\mathcal{F}_X(C_k^l) = \sum_{e \in \mathcal{E}^X} \Xi(e, C_k^l) \mathcal{F}_e, \quad (19)$$

$$\mathcal{F}_Y(C_k^l) = \sum_{e \in \mathcal{E}^Y} \Xi(e, C_k^l) \mathcal{F}_e. \quad (20)$$

Note that the partial affinities are found to be as dissimilar as  $\mathcal{F}(C_k^l)$ , because the sums are not taken over  $\mathcal{E}$  but over  $\mathcal{E}^X$  and  $\mathcal{E}^Y$ .

By using the definition in Eq. (14), one can also define the effective affinity of  $C_k^l$  by

$$\mathcal{F}(C_k^l) := \sum_{e \in \mathcal{E}} \Xi(e, C_k^l) \mathcal{F}_e. \quad (21)$$

The partial effective affinities of the cycles corresponding to  $X$  and  $Y$  are written as

$$\mathcal{F}_X(C_k^l) = \sum_{e \in \mathcal{E}^X} \Xi(e, C_k^l) \mathcal{F}_e, \quad (22)$$

$$\mathcal{F}_Y(C_k^l) = \sum_{e \in \mathcal{E}^Y} \Xi(e, C_k^l) \mathcal{F}_e. \quad (23)$$

Combining Eqs. (21)-(23) with Eqs. (12) and (17), one can obtain the effective affinities of local cycles and the partial effective affinities of the global cycle in Eq. (16)

$$\mathcal{F}(C_1^X) = \mathcal{F}(C_2^X) := -\Delta\mu_X/T, \quad (24)$$

$$\mathcal{F}(C_1^Y) = \mathcal{F}(C_2^Y) := -\Delta\mu_Y/T, \quad (25)$$

$$\mathcal{F}_X(C_1^G) = -\mathcal{F}_Y(C_1^G) = \ln \frac{p(x_0, y_1) p(x_1, y_0)}{p(x_0, y_0) p(x_1, y_1)} - U/T, \quad (26)$$

where  $\Delta\mu_X = \mu_{XR} - \mu_{XL}$  and  $\Delta\mu_Y = \mu_{YR} - \mu_{YL}$ . For the global cycle  $C_1^G$ , the partial affinities  $\mathcal{F}_X(C_1^G) = -\mathcal{F}_Y(C_1^G) = -U/T$ . The partial effective affinities of the global cycle in Eq. (26) is equal to the sum of the two forces, i.e.,

$$\mathcal{F}_X(C_1^G) = \mathcal{F}_X(C_1^G) + \mathcal{F}_I(C_1^G), \quad (27)$$

$$\mathcal{F}_Y(C_1^G) = \mathcal{F}_Y(C_1^G) - \mathcal{F}_I(C_1^G), \quad (28)$$

where  $\mathcal{F}_I(C_1^G) = \ln \frac{p(x_0, y_1)p(x_1, y_0)}{p(x_0, y_0)p(x_1, y_1)}$  provides the driving force for the information exchanges between  $X$  and  $Y$ .

The transitions around cycle  $C_k^l$  generate the net current  $J(C_k^l)$  (cycle current), which is fundamental in irreversible thermodynamics. At steady state, Kirchhoff's laws govern the conservation of energy and charge, indicating that

$$J_e = \sum_{C_k^l \in \mathcal{C}} \Xi(e, C_k^l) J(C_k^l). \quad (29)$$

Therefore, the currents corresponding to the basic cycles [Eq. (16)] can be calculated as

$$\begin{aligned} J(C_1^X) &:= R_{x_0x_1|y_0}^{(XR)} p(x_1, y_0) - R_{x_1x_0|y_0}^{(XR)} p(x_0, y_0) = J_{x_0x_1|y_0}^{(XR)}, \\ J(C_2^X) &:= R_{x_0x_1|y_1}^{(XR)} p(x_1, y_1) - R_{x_1x_0|y_1}^{(XR)} p(x_0, y_1) = J_{x_0x_1|y_1}^{(XR)}, \\ J(C_1^G) &:= \left( R_{y_1y_0|x_0}^{(YL)} + R_{y_1y_0|x_0}^{(YR)} \right) p(x_0, y_0) - \left( R_{y_0y_1|x_0}^{(YL)} + R_{y_0y_1|x_0}^{(YR)} \right) p(x_0, y_1) = J_{y_1y_0|x_0}^{(YL)} + J_{y_1y_0|x_0}^{(YR)}, \end{aligned} \quad (30)$$

$$\begin{aligned} J(C_1^Y) &:= R_{y_0y_1|x_0}^{(YR)} p(x_0, y_1) - R_{y_1y_0|x_0}^{(YR)} p(x_0, y_0) = J_{y_0y_1|x_0}^{(YR)}, \\ J(C_2^Y) &:= R_{y_0y_1|x_1}^{(YR)} p(x_1, y_1) - R_{y_1y_0|x_1}^{(YR)} p(x_1, y_0) = J_{y_0y_1|x_1}^{(YR)}, \end{aligned}$$

where  $J_{xx'|y}^{(\nu)}$  represents the current due to the transition  $(x', y) \xrightarrow{\nu} (x, y)$ , and similarly for  $J_{yy'|x}^{(\nu)}$ .

The net electronic currents from  $XR$  and  $XL$  and from  $YR$  and  $YL$  are, respectively, simplified as

$$J_X = - (J(C_1^X) + J(C_2^X)), \quad (31)$$

$$J_Y = - (J(C_1^Y) + J(C_2^Y)). \quad (32)$$

#### D. Nonequilibrium Clausius inequalities of the two subsystems

Given the probability of a microstate, the entropy of the system is as follows [17, 42, 43]

$$S(t) = - \sum_z p(z, t) \ln p(z, t). \quad (33)$$

For steady states, the time derivative of Eq. (33) reduces to

$$\dot{S} = \dot{\sigma} + \dot{S}_r = 0, \quad (34)$$

where

$$\dot{\sigma} = \sum_{\nu} \sum_{z, z'} R_{zz'}^{(\nu)} p(z', t) \ln \frac{R_{zz'}^{(\nu)} p(z', t)}{R_{z'z}^{(\nu)} p(z, t)} \quad (35)$$

is the rate of total entropy production [44], and

$$\dot{S}_r = - \sum_{\nu} \sum_{z, z'} R_{zz'}^{(\nu)} p(z', t) \ln \frac{R_{zz'}^{(\nu)}}{R_{z'z}^{(\nu)}} \quad (36)$$

describes the the entropy flow from reservoirs.

The Logarithmic sum inequality states that for non-negative  $a_i$  and  $b_i$ ,  $\sum_{i=1}^n a_i \ln \frac{a_i}{b_i} \geq a \ln \frac{a}{b}$  with  $a = \sum_i a_i$  and  $b = \sum_i b_i$ . Therefore, one can prove that  $\dot{\sigma} \geq 0$  and the second law of thermodynamics holds for the system. In the long time limit, the system reaches an unique non-equilibrium stationary state and  $\dot{S} = 0$ . The rate of entropy production must be balanced by the entropy flows through its terminals, i.e.,  $\dot{\sigma} = -\dot{S}_r$ .

The transition rates [Eq. (11)] between different states satisfy the local detailed balance, e.g.,  $\ln \frac{R_{x_1 x_0 | y_0}^{(XR)}}{R_{x_0 x_1 | y_0}^{(XR)}} = -(\varepsilon'_X - \mu_{XR})/T$  and  $\ln \frac{R_{x_1 x_0 | y_1}^{(XR)}}{R_{x_0 x_1 | y_1}^{(XR)}} = -(\varepsilon'_X + U - \mu_{XR})/T$ . Thus, the entropy flow is simplified as

$$\dot{S}_r = - [J_X \Delta \mu_X + J_Y \Delta \mu_Y] / T. \quad (37)$$

For the interaction between  $X$  and reservoir  $XR$ ,  $\varepsilon'_X - \mu_{XR}$  and  $\varepsilon'_X + U - \mu_{XR}$  represent the thermal energies supplied by reservoir  $XR$  during a jump in the subsystem  $X$ , which enables us to identify the heat currents into  $X$  from reservoir  $XR$

$$\begin{aligned} \dot{Q}_{XR} &= T \left( J_{x_0 x_1 | y_0}^{(XR)} \ln \frac{R_{x_1 x_0 | y_0}^{(XR)}}{R_{x_0 x_1 | y_0}^{(XR)}} + J_{x_0 x_1 | y_1}^{(XR)} \ln \frac{R_{x_1 x_0 | y_1}^{(XR)}}{R_{x_0 x_1 | y_1}^{(XR)}} \right) \\ &= -J_{x_0 x_1 | y_0}^{(XR)} (\varepsilon'_X - \mu_{XR}) - J_{x_0 x_1 | y_1}^{(XR)} [(\varepsilon'_X + U - \mu_{XR})]. \end{aligned} \quad (38)$$

By following the same path, the heat currents into the system from reservoirs  $XL$ ,  $YR$ , and  $YL$  are, respectively, given by

$$\dot{Q}_{XL} = J_{x_1x_0|y_0}^{(XL)} (\varepsilon'_X - \mu_{XL}) + J_{x_1x_0|y_1}^{(XL)} (\varepsilon'_X + U - \mu_{XL}), \quad (39)$$

$$\dot{Q}_{YR} = -J_{y_0y_1|x_0}^{(YR)} (\varepsilon'_Y - \mu_{YR}) - J_{y_0y_1|x_1}^{(YR)} (\varepsilon'_Y + U - \mu_{YR}), \quad (40)$$

and

$$\dot{Q}_{YL} = J_{y_1y_0|x_0}^{(YL)} (\varepsilon'_Y - \mu_{YL}) + J_{y_1y_0|x_1}^{(YL)} (\varepsilon'_Y + U - \mu_{YL}). \quad (41)$$

The rate of total entropy production can be conveniently related to the heat currents by summing up Eqs. (38)-(41), i.e.,

$$\dot{\sigma} = -\dot{S}_r = -\sum_{\nu} \dot{Q}_{\nu}/T \geq 0. \quad (42)$$

Equations (33)-(37) exclusively explain the entropy flow between the system and the environment. To clarify how energy and information are exchanged between the two subsystems, we introduce the rates of partial entropy production associated with  $X$  and  $Y$  as [8, 45]

$$\dot{\sigma}_X = \sum_{\nu} \sum_{x \geq x', y} J_{xx'|y}^{(\nu)} \ln \frac{R_{xx'|y}^{(\nu)} p(x', y)}{R_{x'x|y}^{(\nu)} p(x, y)}, \quad (43)$$

$$\dot{\sigma}_Y = \sum_{\nu} \sum_{x, y \geq y'} J_{yy'|x}^{(\nu)} \ln \frac{R_{yy'|x}^{(\nu)} p(x, y')}{R_{y'y|x}^{(\nu)} p(x, y)}, \quad (44)$$

where the rate of total entropy production is then divided into two separate parts followed by

$$\dot{\sigma} = \dot{\sigma}_X + \dot{\sigma}_Y. \quad (45)$$

These classification can be proved directly from the relation  $\sum_{z'} J_e = \sum_{\nu, x'} J_{xx'|y}^{(\nu)} + \sum_{\nu, y'} J_{yy'|x}^{(\nu)}$  and the prescribed transition rate [Eq. (10)]. The logarithmic sum inequality again shows that  $\dot{\sigma}_X$  and  $\dot{\sigma}_Y$  are nonnegative individually, i.e.,

$$\dot{\sigma}_X \geq 0, \quad \dot{\sigma}_Y \geq 0, \quad (46)$$

which is a generalized second law of thermodynamics stronger than Eq. (42). Equations (43) and (44) dictating the rate of partial entropy production in each subsystem can be resolved into three components

$$\dot{\sigma}_X = \dot{\sigma}_{\mu_X} + \dot{\sigma}_{U_X} - \dot{I}_X, \quad (47)$$

$$\dot{\sigma}_Y = \dot{\sigma}_{\mu_Y} + \dot{\sigma}_{U_Y} - \dot{I}_Y, \quad (48)$$

where

$$\begin{aligned} \dot{\sigma}_{\mu_X} &= \mathcal{F}(C_1^X) (J(C_1^X) + J(C_2^X)), \\ \dot{\sigma}_{\mu_Y} &= \mathcal{F}(C_1^Y) (J(C_1^Y) + J(C_2^Y)), \\ \dot{\sigma}_{U_X} &= \mathcal{F}_X(C_1^G) J(C_1^G), \\ \dot{\sigma}_{U_Y} &= \mathcal{F}_Y(C_1^G) J(C_1^G), \\ \dot{I}_X &= -J(C_1^G) \mathcal{F}_I(C_1^G), \\ \dot{I}_Y &= J(C_1^G) \mathcal{F}_I(C_1^G). \end{aligned} \quad (49)$$

The first term  $\dot{\sigma}_{\mu_{X(Y)}}$  indicates that the local cycle  $C_k^{X(Y)}$  having a local affinity  $\mathcal{F}(C_k^{X(Y)})$  supports the internal flows within the subsystem. The global cycle  $C_1^G$  generates a global current  $J(C_1^G)$  to carry the energy and information from one subsystem to the other.  $\dot{\sigma}_{U_X}$  and  $\dot{\sigma}_{U_Y}$  are responsible for the direct energy transfer between  $X$  and  $Y$  due to the Coulomb coupling. Any energy extracted by the partial affinity  $\mathcal{F}_X(C_1^G)$  will be deposited in  $Y$ 's environment by  $\mathcal{F}_Y(C_1^G)$ . The information flow  $\dot{I}_{X(Y)}$  exclusively occurs on the global cycle  $C_1^G$  with information affinity  $\mp \mathcal{F}_I(C_1^G)$ . When  $\mathcal{F}_X(C_1^G) \ll \mathcal{F}_I(C_1^G)$ , the dominant force for driving  $X$  is information. On the other hand, when  $\mathcal{F}_X(C_1^G) \gg \mathcal{F}_I(C_1^G)$ , the interaction is mainly powered by energy. The cycle graph analysis enables a better understanding of the driving mechanisms of the internal interactions.

### E. Nonequilibrium free energy inequalities of the two subsystems

Since  $\mathcal{F}(C_1^{X(Y)})$  takes the chemical potential difference as the thermodynamic driving force and  $J(C_1^{X(Y)}) + J(C_2^{X(Y)})$  represents the net electronic current along  $X(Y)$ , the work flux  $\dot{W}_{X(Y)}$  performed on a subsystem is identified as

$$\dot{W}_{X(Y)} = T \mathcal{F}(C_1^{X(Y)}) \left[ J(C_1^{X(Y)}) + J(C_2^{X(Y)}) \right] = -T \mathcal{F}(C_1^{X(Y)}) J_{X(Y)}. \quad (50)$$

According to the first law of thermodynamics, the energy flow  $\dot{E}_{X(Y)}$  into the subsystem reads

$$\begin{aligned}\dot{E}_{X(Y)} &= \dot{Q}_{X(Y)L} + \dot{Q}_{X(Y)R} + \dot{W}_{X(Y)} \\ &= -T\mathcal{F}_{X(Y)}(C_1^G) J(C_1^G),\end{aligned}\tag{51}$$

depending on the Coulomb force and the global current. The steady-state internal energy of the bipartite system remains constant ( $d_t E = \dot{E}_X + \dot{E}_Y = 0$ ). Multiplying Eq. (46) by  $T$  and applying the above derivatives, one gets

$$T\dot{\sigma}_{X(Y)} = \dot{W}_{X(Y)} - \dot{F}_{X(Y)} \geq 0,\tag{52}$$

where the rate of partial nonequilibrium free energy  $\dot{F}_{X(Y)}$  associated with  $X$  ( $Y$ ) is defined as [21, 23]

$$\dot{F}_{X(Y)} = \dot{E}_{X(Y)} + T\dot{I}_{X(Y)}.\tag{53}$$

Equation (52) provides an extension of the second law of thermodynamics. From a practical point of view, it means that the total amount of work that can be extracted in the nonequilibrium system is limited by the decrease of free energy. The rate of partial nonequilibrium free energy can be partitioned into the information-related and energy-related parts. Its definition has been generally found appropriately, because  $\dot{I}_{X(Y)}$  is equivalent to the rate of the Shannon entropy of the system  $\dot{S}$  due to the interaction with the reservoirs  $XL$  ( $YL$ ) and  $XR$  ( $YR$ ).

### III. RESULTS AND DISCUSSION

Without loss of generality, we control over the tunnel rate in the weak coupling regime. For characterizing the Coulomb blocking effect, the parameters of the potential barriers are chosen as follows:  $\Gamma_{x_0}^{(XL)} = \Gamma_{\cosh(\delta)}^{e^{+\delta}}$ ,  $\Gamma_{x_1}^{(XL)} = \Gamma_{\cosh(\delta)}^{e^{-\delta}}$ ,  $\Gamma_{x_0}^{(XR)} = \Gamma_{\cosh(\delta)}^{e^{-\delta}}$ ,  $\Gamma_{x_1}^{(XR)} = \Gamma_{\cosh(\delta)}^{e^{+\delta}}$ ,

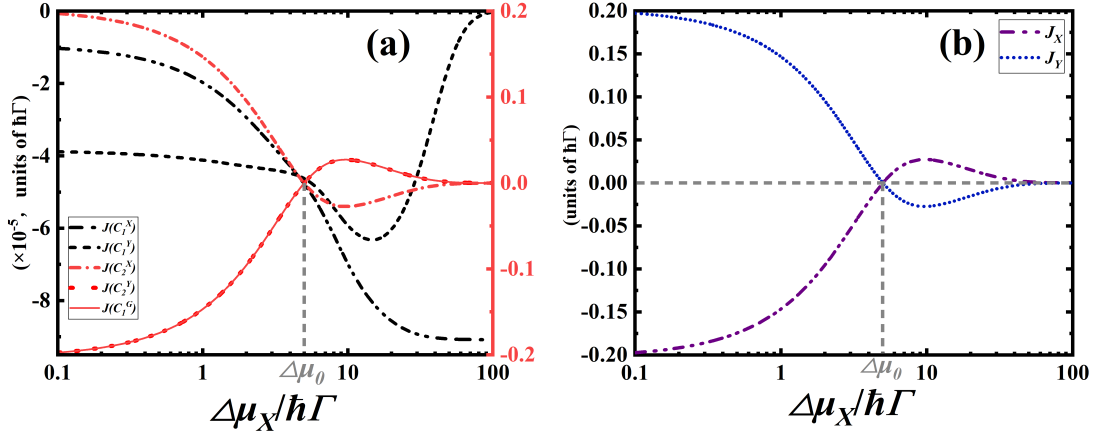


Figure 3: The curves of (a) the cycle currents and (b) the electronic currents  $J_X$  and  $J_Y$  varying with the chemical potential difference  $\Delta\mu_X/\hbar\Gamma$ . The left vertical axis shows the values for  $J(C_1^X)$  and  $J(C_2^X)$ , while the corresponding scales of  $J(C_1^G)$ ,  $J(C_1^Y)$ , and  $J(C_2^Y)$  are on the right vertical axis. The parameters  $\varepsilon_X = 0$ ,  $\varepsilon_Y = 0$ ,  $\Delta\mu_Y = 5.0\hbar\Gamma$ ,  $\mu_{XL} - \mu_{YL} = 1.0\hbar\Gamma$ ,  $C = 0.5q^2/\hbar\Gamma$ ,  $C_0 = 1.0q^2/\hbar\Gamma$ ,  $k_B T = 1.0\hbar\Gamma$ , and  $\Delta = \delta = 5.0$ . These values are used unless otherwise mentioned specifically in the following discussion.

$\Gamma_{y_0}^{(YL)} = \Gamma \frac{e^{+\Delta}}{\cosh(\Delta)}$ ,  $\Gamma_{y_1}^{(YL)} = \Gamma \frac{e^{-\Delta}}{\cosh(\Delta)}$ ,  $\Gamma_{y_0}^{(YR)} = \Gamma \frac{e^{-\Delta}}{\cosh(\Delta)}$ , and  $\Gamma_{y_1}^{(YR)} = \Gamma \frac{e^{+\Delta}}{\cosh(\Delta)}$ . In addition, we set  $C_{XL} = C_{XR} = C_{YL} = C_{YR} = C_0$ .

Figure 3 (a) shows the currents of the fundamental cycles selected in Eq. (30). When the dot  $Y$  ( $X$ ) is empty, the local cycle current  $J(C_1^X) < 0$  (black dash-double-dotted line) [ $J(C_1^Y) < 0$  (black dashed line)], meaning that electrons are prone to transfer from the higher chemical potential to the lower chemical potential. When  $Y$  is occupied, the local cycle current  $J(C_2^X)$  (red dash-dotted line) through  $X$  does not move in a fixed direction, but is embodied in two situations. The first case is characterized by  $J(C_2^X) > 0$  in the small- $\Delta\mu_X$  regime ( $\Delta\mu_X < \Delta\mu_0$ ), where the electrons transfer from reservoir  $XL$  to reservoir  $XR$  against the thermodynamic force  $-\mathcal{F}(C_2^X)$  due to the Coulomb coupling. The second case is characterized by  $J(C_2^X) < 0$  in the large- $\Delta\mu_X$  regime ( $\Delta\mu_X > \Delta\mu_0$ ), because the thermodynamic force  $-\mathcal{F}(C_2^X)$  dominates the electron transport again. When  $X$  is occupied, the local cycle current  $J(C_2^Y)$  (red dashed line) changes from negative to positive as  $\Delta\mu_X$  increases. When  $\Delta\mu_X$  is large enough, the dot  $X$  may provide enough energy or information

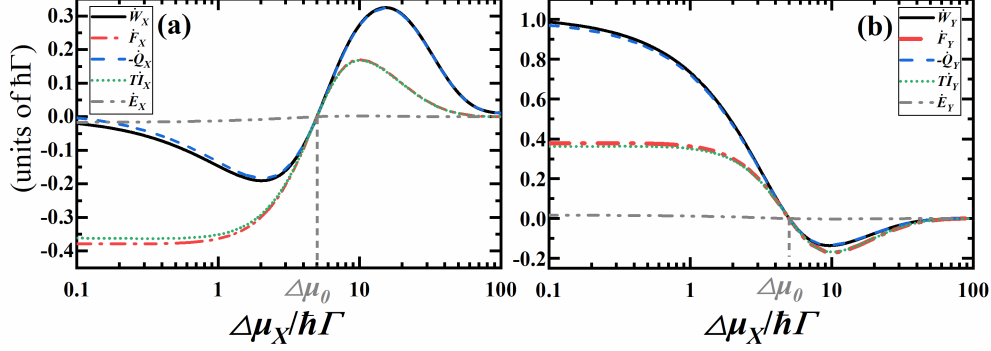


Figure 4: The work fluxes (black solid lines), rates of partial nonequilibrium free energy (red dash-dotted lines), heat currents (blue dashed lines), information flows (green dotted lines), and energy flows (grey dash-double-dotted lines) of the subsystems (a)  $X$  and (b)  $Y$  varying with the chemical potential difference  $\Delta\mu_X/\hbar\Gamma$  at steady state.

for driving the electron flow in the direction opposite to the chemical potential gradient  $-\mathcal{F}(C_2^Y)$ . The graph theory offers an effective way to unearthing the fundamental path, where the current through one dot could drag the current through the other dot.

In the regime of small  $\Delta\mu_X$ , the direction of the global cycle current is counterclockwise  $J(C_1^G) < 0$ . According to Eq. (51), multiplying  $J(C_1^G)$  by the partial affinities  $-\mathcal{F}_X(C_1^G)$  and  $-\mathcal{F}_Y(C_1^G)$ , respectively, we know that the energy flow is fed from  $X$  to  $Y$  (grey dash-double-dotted lines Fig. 4). In the latter, the direction of the global cycle current becomes clockwise as  $\Delta\mu_X$  increases, which lies the regime suitable for the energy flowing from  $Y$  to  $X$ . By applying Eqs. (31) and (32), Fig. 3 (b) presents the net electronic currents from  $XR$  to  $XL$  ( $J_X$ ) and from  $YR$  to  $YL$  ( $J_Y$ ). Owing to the existence of electron-electron interaction, the local cycle current  $J(C_2^X)$  [ $J(C_2^Y)$ ] makes a major contribution to the currents  $J_X$  ( $J_Y$ ). For  $\Delta\mu_X < \Delta\mu_0$ , the net electronic current  $J_X$  flows from the reservoir  $XL$  with the lower chemical potential to the reservoir  $XR$  with the higher chemical potential. The work flux  $\dot{W}_X < 0$  (black solid line in Fig. 4), so that the dot  $X$  produces power output. As  $\Delta\mu_X$  gets larger, the situation is exactly the opposite. The net electronic current  $J_Y$  flows against the bias due to the thermodynamic force and the dot  $Y$  starts to generate positive power output.

The currents of the fundamental cycles are more important to investigate the thermo-

dynamics of the rates of the partial nonequilibrium free energy (red dash-dotted lines) and information flows (green dotted lines). The nonequilibrium Clausius and free energy inequalities [Equations (46) and (52)] serve the subsystems with the local second law of thermodynamics, which are demonstrated in Fig. 4. They behave equivalently and complement each other for a unify treatment of temperature. For  $\Delta\mu_X < \Delta\mu_0$ , the total heat current into  $X$ ,  $\dot{Q}_X = \dot{Q}_{XR} + \dot{Q}_{XL} > 0$ . To achieve this effect, a noticeable information flowing from  $Y$  to  $X$  guarantees that  $T\dot{\sigma}_X = -\dot{Q}_X - T\dot{I}_X > 0$ . The information flow benefits from the current of the global cycle  $J(C_1^G)$  driven by the information affinity  $\mathcal{F}_I(C_1^G)$ . At the same time, the dot  $X$  performs work  $\dot{W}_X < 0$ , which is enabled by the negative rate of partial nonequilibrium free energy  $0 > \dot{W}_X > \dot{F}_X$ . Note that these effects are compensated by the dissipation of work into heat in the dot  $Y$ . For  $\Delta\mu_X > \Delta\mu_0$ , the roles of  $X$  and  $Y$  are totally reversed. It should be emphasized that under most conditions the power output is generated due to the feedback-induced information flow and not due to energy flow, because  $\dot{E}_{X(Y)} \approx 0$  and  $\dot{F}_{X(Y)} \approx T\dot{I}_{X(Y)}$ . As a result, the nonequilibrium double quantum-dot system works as a quantum autonomous Maxwell demon.

#### IV. CONCLUSIONS

In summary, the present work reveals the local second law of thermodynamics of the Coulomb-coupled double quantum dots. The graph theory has proved that the entropy production and nonequilibrium free energy are close related to the information flow and affinities. The information flow between the subsystems acts as a driving force for the global cycle to pump electrons against the bias voltage. The proposed model offers possible schemes to design nanoelectronic devices through the control of cycle fluxes.

#### Acknowledgments

This work has been supported by the National Natural Science Foundation (Grant No. 11805159), the Fundamental Research Fund for the Central Universities (No. 20720180011),

and the Natural Science Foundation of Fujian Province of China (No. 2019J05003).

---

- [1] H. B. Callen, *Thermodynamics and an introduction to thermostatistics* (John Wiley & Sons, New York, 1985).
- [2] L. Onsager, *Phys. Rev. B* 37, 405–426 (1931).
- [3] J. Meixner, *Z. Elektrochem. Ber. Bunsenges. Physik. Chem.* 66, 883–884 (1962).
- [4] G. Benenti, G. Casati, K. Saito, and R. S. Whitney, *Phys. Rep.* 694, 1–124 (2017).
- [5] J. Ren, *Front. Phys.* 12, 120505 (2017).
- [6] F. Ramirez, *Q. Rev. Biol.* 53, 303–304 (1978).
- [7] F. Zhang, L. Xu, K. Zhang, E. Wang, and J. Wang, *J. Chem. Phys.* 137, 065102 (2012).
- [8] J. M. Horowitz and M. Esposito, *Phys. Rev. X* 4, 031015 (2014).
- [9] S. Yamamoto, S. Ito, N. Shiraishi, and T. Sagawa, *Phys. Rev. E* 94, 052121 (2016).
- [10] U. Seifert, *Rep. Prog. Phys.* 75, 126001 (2012).
- [11] M. Einax and A. Nitzan, *J. Chem. Phys.* 145, 014108 (2016).
- [12] D. Andrieux and P. Gaspard, *J. Stat. Phys.* 127, 107–131 (2007).
- [13] N. Taniguchi, *Phys. Rev. B* 97, 155404 (2018).
- [14] J. Anders and M. Esposito, *New J. Phys.* 19, 010201 (2017).
- [15] G. E. Crooks, *J. Stat. Phys.* 90, 1481–1487 (1998).
- [16] G. E. Crooks, *Phys. Rev. E* 60, 2721–2726 (1999).
- [17] M. Esposito, U. Harbola, and S. Mukamel, *Rev. Mod. Phys.* 81, 1665–1702 (2009).
- [18] S. Vaikuntanathan and C. Jarzynski, *Phys. Rev. Lett.* 100, 190601 (2008).
- [19] C. Jarzynski, *Phys. Rev. Lett.* 78, 2690–2693 (1997).
- [20] G. Huber, F. Schmidt-Kaler, S. Deffner, and E. Lutz, *Phys. Rev. Lett.* 101, 070403 (2008).
- [21] M. Esposito and C. Van den Broeck, *Europhys. Lett.* 95, 40004 (2011).
- [22] M. Esposito, K. Lindenberg, and C. Van den Broeck, *New J. Phys.* 12, 013013 (2010).
- [23] K. Ptaszyński and M. Esposito, *Phys. Rev. Lett.* 122, 150603 (2019).
- [24] S. Deffner and C. Jarzynski, *Phys. Rev. X* 3, 041003 (2013).
- [25] P. Talkner, M. Campisi, and P. Hänggi, *J. Stat. Mec. Theor. Exp.* 2009, P02025 (2009).
- [26] H. Miyahara and K. Aihara, *Phys. Rev. E* 98, 042138 (2018).
- [27] T. Sagawa and M. Ueda, *Phys. Rev. Lett.* 104, 090602 (2010).

- [28] A. C. Barato and U. Seifert, *Phys. Rev. Lett.* 112, 090601 (2014).
- [29] Y. Morikuni and H. Tasaki, *J. Stat. Phys.* 143, 1–10 (2011).
- [30] J. M. Horowitz and H. Sandberg, *New J. Phys.* 16, 125007 (2014).
- [31] J. M. Horowitz, *J. Stat. Mech. Theor. Exp.* 2015, P03006 (2015).
- [32] A. Chapman and A. Miyake, *Phys. Rev. E* 92, 062125 (2015).
- [33] A. Soltanmanesh and A. Shafiee. *Eur. Phys. J. Plus* 134, 282 (2019).
- [34] U. M. B. Marconi, A. Puglisi, and C. Maggi, *Sci. Rep.* 7, 46496 (2017).
- [35] L. Bertini, A. De Sole, D. Gabrielli, G. Jona-Lasinio, and C. Landim, *J. Stat. Mech. Theor. Exp.* 2015, P10018 (2015).
- [36] Y. Zhang, C. Huang, J. Wang, G. Lin, and J. Chen, *Energy* 85, 200–207 (2015).
- [37] R. Sánchez and M. Büttiker, *Phys. Rev. B* 83, 085428 (2011).
- [38] C. W. J. Beenakker, *Phys. Rev. B* 44, 1646–1656 (1991).
- [39] D. V. Averin, A. N. Korotkov, and K. K. Likharev, *Phys. Rev. B* 44, 6199–6211 (1991).
- [40] S. Nakajima and Y. Tokura, *J. Stat. Phys.* 169, 902–928 (2017).
- [41] J. Schnakenberg, *Rev. Mod. Phys.* 48, 571–585 (1976).
- [42] H. Spohn, *J. Math. Phys.* 19, 1227–1230 (1978).
- [43] M. Esposito, U. Harbola, and S. Mukamel, *Phys. Rev. E* 76, 031132 (2007).
- [44] G. Schaller, *Open Quantum Systems Far from Equilibrium* (Springer, New York, 2014).
- [45] N. Shiraishi and T. Sagawa, *Phys. Rev. E* 91, 012130 (2015).